Visual Feedback Attitude Synchronization: Tracking Performance Analysis

Tatsuya Ibuki

FL10-15-1

26th, October, 2010

Introduction

Mobile Sensor Network

A network consisting of multiple mobile sensors or robots with sensing devices

Network : Performance or Robustness against failures

Mobile : Dynamical environments

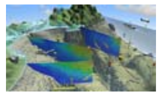
Environmental Monitoring

Applications

- Environmental Monitoring
- Search
- Exploration and Mapping
- Management System of Infrastructure


Oceanic Pollution

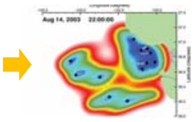
Ocean Sampling

Operation of Mobile Sensor Network

Each sensor is required to act cooperatively using only limited information.

Cooperative Control

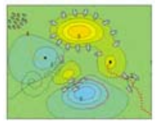
Cooperative Control

Introduction

Cooperative Control of Robotic Network

A distributed control strategy using only local information so that the robotic network achieves specified tasks

Cooperative Control Problems for Mobile Sensor Network

formulated as

Pose Coordination Problems

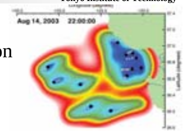
Ocean Sampling

Attitude Synchronization

To lead all agents' attitudes to a common one by utilizing distributed control strategies

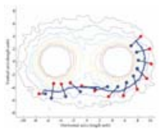
Pose Coordination

Available Information

Only Visual Information: each agent has vision

Objective of Our Work

To present vision-based attitude synchronization control laws for robotic networks in 3-dimensional space, prove the convergence mathematically and analyze the performance.

Outline

- Introduction
- Visual Robotic Network
  - Rigid Body Motion
  - Visibility Structure
  - Measured Output
- Visual Feedback Attitude Synchronization
- Tracking Performance
- Simulation
- Conclusion and Future Works

Visual Robotic Network: Rigid Body Motion

Kinematics of Rigid Bodies

Pose $(p_{wi}, e^{\hat{\xi}\theta_{wi}}) \in SE(3)$

$$g_{wi} = \begin{bmatrix} e^{\hat{\xi}\theta_{wi}} & p_{wi} \\ 0 & 1 \end{bmatrix} \in \mathcal{R}^{4\times 4}$$

Exponential Coordinate for Rotation

$\xi_{wi} \in \mathcal{R}^3$: rotation axis

$\theta_{wi} \in \mathcal{R}$: rotation angle

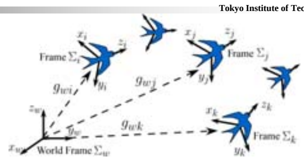

$p_{wi} \in \mathcal{R}^3$: position

$e^{\hat{\xi}\theta_{wi}} \in \mathcal{R}^{3\times 3}$: attitude

$\wedge$: $\begin{bmatrix} \omega_x \\ \omega_y \\ \omega_z \end{bmatrix}^{\wedge} = \begin{bmatrix} 0 & -\omega_z & \omega_y \\ \omega_z & 0 & -\omega_x \\ -\omega_y & \omega_x & 0 \end{bmatrix}$

$\vee$: Inverse Operator of $\wedge$

Body Velocity

Common $(v_{wi}^b = v_{wj}^b \ {}^\forall i, j)$

$$V_{wi}^b = \begin{bmatrix} v_{wi}^b \\ \omega_{wi}^b \end{bmatrix} \in \mathcal{R}^6 \qquad \hat{V}_{wi}^b = \begin{bmatrix} \hat{\omega}_{wi}^b & v_{wi}^b \\ 0 & 0 \end{bmatrix} \in \mathcal{R}^{4\times 4}$$

Control Input $\quad (:= g_{wi}^{-1}\dot{g}_{wi})$

$v_{wi}^b \in \mathcal{R}^3$: linear velocity

$\omega_{wi}^b \in \mathcal{R}^3$: angular velocity

Rigid Body Motion

$$\boxed{\dot{g}_{wi} = g_{wi}\hat{V}_{wi}^b \quad (1)}$$

Relative Rigid Body Motion

$$V_{ij}^b := (g_{ij}^{-1}\dot{g}_{ij})^{\vee} = -\mathrm{Ad}_{(g_{ij}^{-1})}V_{wi}^b + V_{wj}^b \quad (2)$$

$\mathrm{Ad}_{(g_{ij}^{-1})} \in \mathcal{R}^{6\times 6}$: coordi. trans. from Σ_{wi} to Σ_{wj}

$g_{ij} := g_{wi}^{-1}g_{wj} = (p_{ij}, e^{\hat{\xi}\theta_{ij}})$: pose of rigid body j relative to body i

Visual Robotic Network: Visibility Structure and Measured Output

Visibility Structure among Rigid Bodies

Rigid Body Set $\quad$ Visibility Set

$\mathcal{V} := \{1, \cdots, n\} \qquad \mathcal{E} \subset \mathcal{V} \times \mathcal{V}$ $\left[(j, i) \in \mathcal{E}\text{: body } j \text{ is visible from body } i\right]$

Visible Bodies

$$\boxed{\mathcal{N}_i := \{j \in \mathcal{V} \mid (j, i) \in \mathcal{E}\} \quad (3)}$$

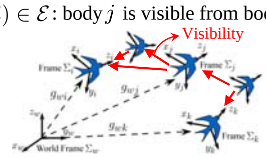

Measured Output

$$\boxed{f_i = (f_{ij})_{j\in\mathcal{N}_i} \quad (4)} \qquad f_{ij} := [f_{ij_1}^T \ \cdots \ f_{ij_m}^T]^T \in \mathcal{R}^{2m}$$

Vision Model (Perspective Projection)

$$f_{ij_k} = \frac{\lambda_i}{z_{ij_k}}\begin{bmatrix} x_{ij_k} \\ y_{ij_k} \end{bmatrix} \in \mathcal{R}^2 \quad \lambda_i \in \mathcal{R}\text{: focal length}, \ k \in \{1, \cdots, m\}$$

$$p_{ij_k} = \begin{bmatrix} x_{ij_k} \\ y_{ij_k} \\ z_{ij_k} \end{bmatrix}$$: position of k th feature point of body j relative to body i

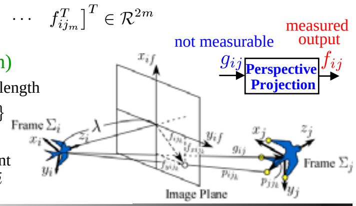

Visual Robotic Network

Visual Robotic Network $\boldsymbol{\Sigma}$

n Rigid Bodies

$$\dot{g}_{wi} = g_{wi}\hat{V}^b_{wi},\ i \in \mathcal{V} \quad (1)$$

Measured Output

$$f_i = (f_{ij})_{j\in\mathcal{N}_I},\ i \in \mathcal{V} \quad (4)$$

Visibility Structure

$$\mathcal{N}_i := \{j \in \mathcal{V} \mid (j,i) \in \mathcal{E}\},\ i \in \mathcal{V} \quad (3)$$

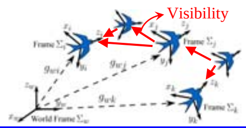

Assumption 1 (Leader-following Type Visibility Structure)

- there exists a leader which has no visible body $(\mathcal{N}_1 = \emptyset)$
- the other bodies have a fixed visible body $(|\mathcal{N}_i| = 1,\ \text{and}\ \mathcal{N}_i\ \text{is fixed}\ {}^\forall i \in \mathcal{V}\setminus\{1\})$
- there exists a visibility path from each body to the leader $({}^\forall i \in \mathcal{V}\setminus\{1\},\ {}^\exists v_1,\cdots,v_r \in \mathcal{V}\ s.t.\ v_1 = 1,\ v_r = i$ $(v_k, v_{k+1}) \in \mathcal{E}\ {}^\forall k \in \{1,\cdots,r-1\})$

$G := (\mathcal{V},\mathcal{E})$: Graph

- Graph: Directed Spanning Tree

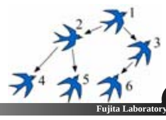

Outline

- Introduction
- Visual Robotic Network
- Visual Feedback Attitude Synchronization
  - Definition of Visual Feedback Attitude Synchronization
  - Visual Feedback Attitude Synchronization Law
  - Convergence Analysis
- Tracking Performance
- Simulation
- Conclusion and Future Works

Visual Feedback Attitude Synchronization

Definition: Visual Feedback Attitude Synchronization

A visual robotic network Σ is said to achieve visual feedback attitude synchronization, if

$$\begin{cases} v^b_{wi} = v^b_{wj} \\ \lim_{t\to\infty} \phi(e^{-\hat{\xi}\theta_{wi}}e^{\hat{\xi}\theta_{wj}}) = 0 \end{cases},\ {}^\forall i,j \in \mathcal{V} \quad (5)$$

Energy Function of Rotation

$$\phi(e^{\hat{\xi}\theta_{wi}}) := \frac{1}{2}\mathrm{tr}(I_3 - e^{\hat{\xi}\theta_{wi}}) \geq 0 \quad \left(\phi(e^{\hat{\xi}\theta_{wi}}) = 0 \Leftrightarrow e^{\hat{\xi}\theta_{wi}} = I_3\right)$$

Attitude Synchronization

- All rigid bodies' linear velocity is the same
- All attitudes asymptotically converge to a common value

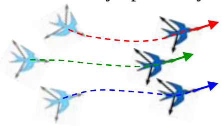

[7] Y. Igarashi, T. Hatanaka, M. Fujita and M. W. Spong, "Passivity-based Attitude Synchronization in SE(3)," *IEEE Trans. on Control System Technology*, Vol. 17, No. 5, pp. 1119-1134, 2009.

Visual Feedback Attitude Synchronization Law

Visual Feedback Attitude Synchronization Law

$$\begin{cases} v^b_{wi} = v \\ \omega^b_{wi} = k_{ij}\mathrm{sk}(\underbrace{e^{\hat{\bar{\xi}}\bar{\theta}_{ij}}}_{\text{Estimated Value}})^\vee \\ \bar{V}^b_{ij} := (\bar{g}^{-1}_{ij}\dot{\bar{g}}_{ij})^\vee = -\mathrm{Ad}_{(\bar{g}^{-1}_{ij})}V^b_{wi} + u_{ij} \\ u_{ij} = k_{eij}\begin{bmatrix} p_{eij} + \frac{1}{k_{eij}}e^{\hat{\xi}\theta_{eij}}v^b_{wi} \\ \mathrm{sk}(e^{\hat{\xi}\theta_{eij}})^\vee - \mathrm{sk}(e^{\hat{\bar{\xi}}\bar{\theta}_{ij}})^\vee \end{bmatrix} \end{cases} \quad (7)$$

Velocity Input (first two equations)

Visual Observer to estimate relative pose of neighbors [10] (last two equations)

$j \in \mathcal{N}_i,\ i \in \mathcal{V}$

$k_{ij}, k_{eij} > 0 \in \mathcal{R}$

$v \in \mathcal{R}^3$: common body linear velocity

$\mathcal{N}_i$: visible bodies

cancel term of velocity input to prove synchronization

Estimated Pose

$$\bar{g}_{ij} = (\bar{p}_{ij}, e^{\hat{\bar{\xi}}\bar{\theta}_{ij}})$$

Estimation Error

$$g_{eij} = \bar{g}^{-1}_{ij}g_{ij} = (p_{eij}, e^{\hat{\xi}\theta_{eij}})$$

$$g_{eij} = I_4 \Rightarrow \bar{g}_{ij} = g_{ij}$$

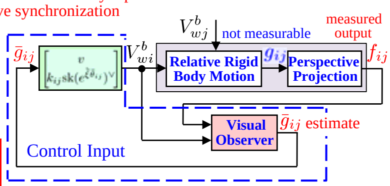

Input (7): calculated only by measured output f_{ij}

[10] M. Fujita, H. Kawai and M. W. Spong, *IEEE Trans. on Control System Technology*, Vol. 15, No. 1, pp. 40-52, 2007.

Visual Feedback Attitude Synchronization

Theorem 1: Visual Feedback Attitude Synchronization

Suppose the leader does not rotate $(\omega^b_{w1} = 0)$. Then, a visual robotic network Σ with control law (7) and Assumption 1 achieves visual feedback attitude synchronization if

$$\begin{cases} k_{jk} < \frac{2k_{ij}k_{eij}}{k_{ij}+k_{eij}},\ k \in \mathcal{N}_j,\ j \in \mathcal{N}_i,\ i \in \mathcal{V}_q \\ k_{jk} < \frac{2k_{ij}k_{eij}}{k_{ij}+2k_{eij}},\ k \in \mathcal{N}_j,\ j \in \mathcal{N}_i,\ i \in \mathcal{V}_r \end{cases} \quad (10)$$

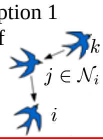

$$\mathcal{V}_q := \{i \in \mathcal{V} \mid i \notin \mathcal{N}_j\ {}^\forall j \in \mathcal{V}\},\ \mathcal{V}_r := \{i \in \mathcal{V}\setminus\{1\} \mid {}^\exists j \in \mathcal{V},\ i \in \mathcal{N}_j\}$$

Gain condition (10) implies that if the backward rigid bodies move fast, then visual feedback attitude synchronization is achieved.

Sketch of Proof

Lyapunov Function Candidate: $q_i = \{1,2,\cdots\}$

$$U := \sum_{i=2}^{n}\sum_{j\in\mathcal{N}_i} q_i\left(\underbrace{\phi(e^{\hat{\bar{\xi}}\bar{\theta}_{ij}})}_{\text{Control}} + \underbrace{\frac{1}{2}\|p_{eij}\|^2_2 + \phi(e^{\hat{\xi}\theta_{eij}})}_{\text{Estimation}}\right) \geq 0$$

⇒ Lyapunov Argument (Asymptotic Stability)

Outline

- Introduction
- Visual Robotic Network
- Visual Feedback Attitude Synchronization
- Tracking Performance
  - Tracking Performance based on Input-to-state Stability
  - Tracking Performance based on $\mathcal{L}_2$ -gain Performance
- Simulation
- Conclusion and Future Works

Tracking Performance Analysis

Theorem 1: $\omega_{w1}^b = 0$

➡ For a rotating leader $(\omega_{w1}^b \neq 0)$, is there sufficient tracking performance ?

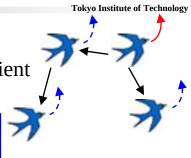

Evaluate attitude errors regarding the leader's angular velocity as an external disturbance

x_e : All rigid bodies' control and estimation errors

Qualitative Evaluation: Input-to-state Stability

For any bounded input, the state will be bounded

$$\|x_e(t)\|_2 \le \beta(\|x_0\|_2, t) + \alpha(\|\omega_{w1}^b\|_{\mathcal{L}_\infty}),\ {}^\forall t \ge 0 \qquad \alpha(\cdot) \in \mathcal{K},\ \beta(\cdot,\cdot) \in \mathcal{KL}$$

Quantitative Evaluation: $\mathcal{L}_2$-gain Performance Analysis

For any energy bounded input, the output will be bounded

$$\|x_e\|_{\mathcal{L}_2} \le \gamma \|\omega_{w1}^b\|_{\mathcal{L}_2} + \delta \qquad \gamma,\ \delta \ge 0$$

H. K. Khalil, *Nonlinear Systems*, Third Edition, Prentice Hall, 2002.

Tracking Performance Analysis based on ISS

Theorem 2: Tracking Performance based on ISS

Suppose the leader rotates $(\omega_{w1}^b \neq 0)$ and Assumption 1 is satisfied. If $|\bar{\theta}_{ij}(0)| < \frac{\pi}{2},\ |\theta_{eij}(0)| < \frac{\pi}{2},\ j \in \mathcal{N}_i,\ i \in \mathcal{V}$ and for any positive scalars $\epsilon_i,\ \epsilon_i'\ (\epsilon_i' > \epsilon_i)$, inequality (12) is satisfied, then there exists class-$\mathcal{KL}$ function $\beta(\cdot,\cdot)$ and class-$\mathcal{K}$ function $\alpha(\cdot)$ satisfying inequality (13).

$$\begin{cases} k_{eij} > \epsilon_i \\ \frac{k_{eij}(k_{ij}-\epsilon_i)}{k_{ij}+k_{eij}-\epsilon_i} > \epsilon_i' \end{cases},\ j \in \mathcal{N}_i,\ i \in \mathcal{V}, \quad (12)$$

$$\|x_e(t)\|_2 \le \beta(\|x_e(0), t\|_2) + \alpha(\|\omega_{w1}^b\|_{\mathcal{L}_\infty}). \quad (13)$$

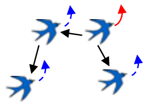

Control Error Vector: $e_{cij} = \mathrm{sk}(e^{\hat{\xi}\bar{\theta}_{ij}})^\vee$

Estimation Error Vector: $e_{ij} = \begin{bmatrix} p_{eij} \\ \mathrm{sk}(e^{\hat{\xi}\theta_{eij}})^\vee \end{bmatrix}$

Error Vector: $e_{ceij} = \begin{bmatrix} e_{cij} \\ e_{ij} \end{bmatrix}$

x_e : Stack Vector of $e_{ceij},\ j \in \mathcal{N}_i,\ i \in \mathcal{V}$

Tracking Performance Analysis based on ISS

Proof

Step 1: 2 rigid bodies

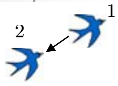

Energy Function: $U_2 := \phi(e^{\hat{\xi}\bar{\theta}_{21}}) + \frac{1}{2}\|p_{e21}\|_2^2 + \phi(e^{\hat{\xi}\theta_{e21}})$

Time Derivative of U_2

$$\dot{U}_2 = -e_{ce21}^T Q_{21} e_{ce21} + e_{e21}^T \omega_{w1}^b \qquad Q_{21} := \begin{bmatrix} (k_{21}+k_{e21})I_3 & -k_{e21}\bar{I} \\ -k_{e21}\bar{I}^T & k_{e21}I_6 \end{bmatrix} \in \mathcal{R}^{9\times 9}$$

Here, $\qquad \bar{I} := [0\ I_3]$

$$e_{e21}^T\omega_{w1}^b = \underbrace{-\frac{\gamma_2}{2}\left\|\omega_{w1}^b - \frac{1}{\gamma_2}e_{e21}\right\|_2^2}_{\le 0} + \frac{\gamma_2}{2}\|\omega_{w1}^b\|_2^2 + \underbrace{\frac{1}{2\gamma_2}\|e_{e21}\|_2^2}_{= e_{ce21}^T W_2 e_{ce21}}$$

$$\left(W_2 := \mathrm{diag}(0_{6\times 6}, \frac{1}{2\gamma_2}I_3)\right)$$

Thus, for any positive scalar ϵ ,

$$\dot{U}_2 \le -e_{ce21}^T Q_{21} e_{ce21} + \frac{\gamma_2}{2}\|\omega_{w1}^b\|_2^2 + e_{ce21}^T W_2 e_{ce21} + \underbrace{\epsilon\|e_{ce21}\|_2^2 - \epsilon\|e_{ce21}\|_2^2}_{=0}$$

$$= -e_{ce21}^T P_2 e_{ce21} + \frac{\gamma_2}{2}\|\omega_{w1}^b\|_2^2 - \epsilon\|e_{ce21}\|_2^2$$

$$(P_2 := Q_{21} - W_2 - \epsilon I_9)$$

Tracking Performance Analysis based on ISS

$$\dot{U}_2 \le \underbrace{-e_{ce21}^T P_2 e_{ce21}}_{\le 0\ \left(\text{Gain Condition (12): } \epsilon' = \frac{1}{2\gamma_2} + \epsilon\right)} + \frac{\gamma_2}{2}\|\omega_{w1}^b\|_2^2 - \epsilon\|e_{ce21}\|_2^2$$

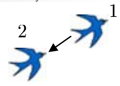

$$\le \frac{\gamma_2}{2}\|\omega_{w1}^b\|_2^2 - \epsilon\|e_{ce21}\|_2^2$$

Integrating from 0 to T yields

$$\underbrace{U_2(T)}_{\ge 0} - U_2(0) \le \frac{\gamma_2}{2}\int_0^T \|\omega_{w1}^b\|_2^2 dt - \epsilon\int_0^T \|e_{ce21}\|_2^2 dt$$

Thus,

$$\int_0^T \|e_{ce21}(t)\|_2^2 dt \le \frac{1}{\epsilon}U_2(0) + \frac{\gamma_2}{2\epsilon}\int_0^T \|\omega_{w1}^b(t)\|_2^2 dt$$

Here, if $|\bar{\theta}_{21}(0)| < \frac{\pi}{2},\ |\theta_{e21}(0)| < \frac{\pi}{2},\ j \in \mathcal{N}_i,\ i \in \mathcal{V}$

$U_2(0) \le \|e_{ce21}(0)\|_2^2$ (Refer to the resume)

Tracking Performance Analysis based on ISS

Thus,

$$\int_0^T \|e_{ce21}(t)\|_2^2 dt \le \frac{1}{\epsilon}\|e_{ce21}(0)\|_2^2 + \frac{\gamma_2}{2\epsilon}\int_0^T \|\omega_{w1}^b(t)\|_2^2 dt$$

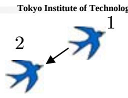

From [16, pp. 95, Theorem 1], we get the following from ISS definition

$$\|e_{ce21}(t)\|_2 \le \beta_2(\|e_{ce21}(0), t\|_2) + \alpha_2(\|\omega_{w1}^b\|_{\mathcal{L}_\infty}) \qquad \alpha_2(\cdot,\cdot) \in \mathcal{K},\ \beta_2(\cdots) \in \mathcal{KL}$$

Step 2: Chain Type Visibility Structure (m Rigid Bodies)

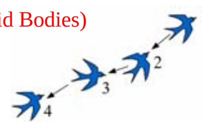

Using the ISS property:

Cascade connection of ISS systems is also ISS

We get the following from ISS definition

$$\|x_{em}(t)\|_2 \le \beta_m(\|x_{em}(0), t\|_2) + \alpha_m(\|\omega_{w1}^b\|_{\mathcal{L}_\infty}) \qquad \alpha_m(\cdot) \in \mathcal{K},\ \beta_m(\cdot,\cdot) \in \mathcal{KL}$$

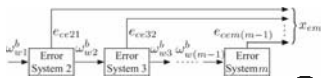

Tracking Performance Analysis based on ISS

Step 3: Multiple Chain Type Visibility Structures (Assumption 1)

For each $\Sigma_{colci},\ i \in \mathcal{V}_q$, we get the following

$$\|x_{ei}(t)\|_2 \le \beta_i(\|x_{ei}(0), t\|_2) + \alpha_i(\|\omega_{w1}^b\|_{\mathcal{L}_\infty}), i \in \mathcal{V}_q$$

$$\alpha_i(\cdot) \in \mathcal{K},\ \beta_i(\cdot,\cdot) \in \mathcal{KL}$$

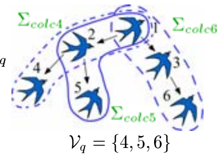

$\mathcal{V}_q = \{4, 5, 6\}$

For $\|\cdot\|_2,\ \beta_i(\cdot,\cdot)$, the followings is satisfied

$$\left\|\begin{matrix} x_{ei} \\ x_{ej} \end{matrix}\right\|_2 \le \|x_{ei}\|_2 + \|x_{ej}\|_2$$

$$\beta_i(\|x_{ei}\|_2, \cdot) + \beta_j(\|x_{ej}\|_2, \cdot) \le \beta_i\left(\left\|\begin{matrix} x_{ei} \\ x_{ej} \end{matrix}\right\|_2, \cdot\right) + \beta_j\left(\left\|\begin{matrix} x_{ei} \\ x_{ej} \end{matrix}\right\|_2, \cdot\right)$$

Thus, summation of the above inequality for $i \in \mathcal{V}_q$ yields

$$\|x_e(t)\|_2 \le \sum_{i\in\mathcal{V}_q}\beta_i(\|x_e(0), t\|_2) + \sum_{i\in\mathcal{V}_q}\alpha_i(\|\omega_{w1}^b\|_{\mathcal{L}_\infty})$$

$\beta := \sum_{i\in\mathcal{V}_q}\beta_i,\ \alpha := \sum_{i\in\mathcal{V}_q}\alpha_i$ ➡ Inequality (13) $\square$

Tracking Performance Analysis based on $\mathcal{L}_2$-gain Performance

Assumption 1 ➡ Multiple Chain Type Visibility Structures

For each $\Sigma_{colci},\ i \in \mathcal{V}_q$

Real Symmetric Matrix: $P_i \in \mathcal{R}^{9(n_i-1)\times 9(n_i-1)}$

(refer to the resume for the definition)

n_i: number of bodies of Σ_{colci}

Identifier: $\{1, 2, \cdots, n_i\}$

$\mathcal{V}_q = \{4, 5, 6\}$

Theorem 3: Tracking Performance based on $\mathcal{L}_2$-gain Performance

Suppose the leader rotates $(\omega_{w1}^b \neq 0)$ and Assumption 1 is satisfied. Then, for any $k_{l(l-1)}, k_{el(l-1)},\ l \in \{2, \cdots, n_i\}$ and positive scalar $\gamma_i,\ i \in \mathcal{V}_q$ satisfying LMI $P_i > 0,\ i \in \mathcal{V}_q$, tshere exists a nonnegative scalar δ satisfying the following inequality.

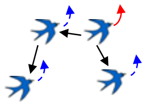

$$\|x_e\|_{\mathcal{L}_2} \leq \gamma \|\omega_{w1}^b\|_{\mathcal{L}_2} + \delta,\ \gamma := \sqrt{\sum_{i\in\mathcal{V}_q} \gamma_i}. \quad (14)$$

γ evaluate cont. and est. errors ➡ Barometer of Tracking Performance

Proof of Theorem 3

Proof

For each $\Sigma_{colci},\ i \in \mathcal{V}_q$

Energy Function: $U_i := \sum_{i=2}^{n_i} \left(\phi(e^{\hat{\xi}\bar{\theta}_{i(i-1)}}) + \frac{1}{2}\|p_{ei(i-1)}\|_2^2 + \phi(e^{\hat{\xi}\theta_{ei(i-1)}}) \right)$

Time Derivative of U_i

$$\dot{U}_i = \underbrace{-x_{ei}^T P_i x_{ei}}_{\leq 0} + \frac{\gamma_i}{2}\|\omega_{w1}^b\|_2^2 - \frac{1}{2}\|x_{ei}\|_2^2 \underbrace{- \frac{\gamma_i}{2}\left\|\omega_{w1}^b - \frac{1}{\gamma_i}x_{ei}\right\|_2^2}_{\leq 0}$$

$$\leq \frac{\gamma_i}{2}\|\omega_{w1}^b\|_2^2 - \frac{1}{2}\|x_{ei}\|_2^2$$

Integrating from 0 to T yields

$$\underbrace{U_i(T) - U_i(0)}_{\geq 0} \leq \frac{\gamma_i}{2}\int_0^T \|\omega_{w1}^b\|_2^2 dt - \frac{1}{2}\int_0^T \|x_i\|_2^2 dt$$

Proof of Theorem 3

$$\underbrace{U_i(T) - U_i(0)}_{\geq 0} \leq \frac{\gamma_i}{2}\int_0^T \|\omega_{w1}^b\|_2^2 dt - \frac{1}{2}\int_0^T \|x_i\|_2^2 dt$$

Summation of the above inequality for $i \in \mathcal{V}_q$ yields

$\left(\|a\|_2^2 + \|b\|_2^2 = \left\|\begin{bmatrix} a \\ b\end{bmatrix}\right\|_2^2\right)$

$$-\sum_{i\in\mathcal{V}_q} U_i(0) \leq \sum_{i\in\mathcal{V}_q} \frac{\gamma_i}{2}\int_0^T \|\omega_{w1}^b(t)\|_2^2 dt - \frac{1}{2}\int_0^T \|x_e(t)\|_2^2 dt$$

Conservative

Extract the square root

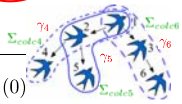

$$\sqrt{\int_0^T \|x_e(t)\|_2^2 dt} \leq \sqrt{\sum_{i\in\mathcal{V}_q}\gamma_i \int_0^T \|\omega_{w1}^b(t)\|_2^2 dt + 2\sum_{i\in\mathcal{V}_q} U_i(0)}$$

Thus, we get the following inequality

$\left(\sqrt{a^2+b^2} \leq a + b\right)$

$$\|x_e\|_{\mathcal{L}_2} \leq \sqrt{\sum_{i\in\mathcal{V}_q}\gamma_i}\|\omega_{w1}^b\|_{\mathcal{L}_2} + \sqrt{2\sum_{i\in\mathcal{V}_q} U_i(0)}$$

$\gamma := \sqrt{\sum_{i\in\mathcal{V}_q}\gamma_i},\ \delta := \sqrt{2\sum_{i\in\mathcal{V}_q} U_i(0)}$ ➡ Inequality (14) □

Analysis of Gain Condition

3 Rigid Bodies $\quad P_3 > 0$

$$P_3 = \begin{bmatrix} \left(k_{21}+k_{e21}-\frac{1}{2}\right)I_3 & 0 & -k_{e21}I_3 & 0 & 0 & -\frac{1}{2}k_{21}I_3 \\ 0 & \left(k_{e21}-\frac{1}{2}\right)I_3 & 0 & 0 & 0 & 0 \\ -k_{e21}I_3 & 0 & \left(k_{e21}-\frac{1}{2}-\frac{1}{2\gamma^2}\right)I_3 & 0 & 0 & 0 \\ 0 & 0 & 0 & \left(k_{32}+k_{e32}-\frac{1}{2}\right)I_3 & 0 & -k_{e32}I_3 \\ 0 & 0 & 0 & 0 & \left(k_{e32}-\frac{1}{2}\right)I_3 & 0 \\ -\frac{1}{2}k_{21}I_3 & 0 & 0 & -k_{e32}I_3 & 0 & \left(k_{e32}-\frac{1}{2}\right)I_3 \end{bmatrix}$$

Q_3, S_3, S_3^T, R_3

Affine on $k_{i(i-1)}, k_{ei(i-1)}$

Schur Complements

$x \in \mathcal{R}^m, Q(x) = Q(x)^T, R(x) = R(x)^T$ and $S(x)$ depend affinely on x.

$$\begin{bmatrix} Q(x) & S(x) \\ S(x)^T & R(x)\end{bmatrix} > 0 \Leftrightarrow \begin{cases} R(x) > 0 \\ Q(x) - S(x)R(x)^{-1}S(x)^T > 0 \end{cases}$$

$$\left(\begin{cases} Q(x) > 0 \\ R(x) - S(x)Q(x)^{-1}S(x)^T > 0 \end{cases} \quad (*)\right)$$

$P_3 := \begin{bmatrix} Q_3(K_3) & S_3(K_3) \\ S_3(K_3)^T & R_3(K_3)\end{bmatrix},\ K_3 := [k_{21}\ k_{e21}\ k_{32}\ k_{e32}]^T$ ➡ $(*)$

S. Boyd, L. E. Ghaoui, E. Feron and V. Balakrishnan, *Linear Matix Inequalities in System and Control Theory*, SIAM Studies in Applied Mathematics, Vol. 15, 1994

Analysis of Gain Condition

$$P_3 > 0 \Leftrightarrow \begin{cases} k_{e21} > \frac{1}{2} \\ \gamma^2 \frac{4k_{21}k_{e21}-2k_{21}-4k_{e21}+1}{2k_{21}+2k_{e21}-1} > 1 \\ k_{e32} > \frac{1}{2} \\ k_{e32} - \frac{1}{2} - \frac{k_{21}^2}{4k_{21}+4k_{e21}-2} - \frac{2k_{e32}^2}{2k_{32}+2k_{e32}-1} \\ \quad - \frac{2\gamma^2 k_{21}^2 k_{e21}^2}{(2k_{21}+2k_{e21}-1)(\gamma^2(4k_{21}k_{e21}-2k_{21}-4k_{e21}+1)-(2k_{21}+2k_{e21}-1))} > 0 \end{cases}$$

too complex

LMI Solutions

Minimize γ Condition: $k_{i(i-1)}, k_{ei(i-1)} < 10$

$k_{21} = 8.72,\ k_{32} = 9.98$

$k_{e21} = 9.97,\ k_{e32} = 9.98$

➡ $\|x_3\|_{\mathcal{L}_2} \leq 0.47\|\omega_{w1}^b\|_{\mathcal{L}_2} + \sqrt{2U_3(0)}$ $(\gamma = 0.47)$

Linear Matrix Inequality

$P_i > 0$

Gain condition or solvability has not found yet.

Outline

- Introduction
- Visual Robotic Network
- Visual Feedback Attitude Synchronization
- Tracking Performance
- Simulation
- Conclusion and Future Works

Simulation

Visibility Structure

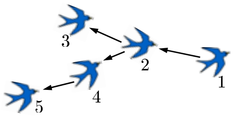

Initial Condition

$p_{w1} = [5\ \ -5\ \ 5]^T$ $\quad \xi\theta_{w1}(0) = \begin{bmatrix}0 & \frac{\pi}{4} & 0\end{bmatrix}^T$

$p_{w2} = [0\ 0\ 0]^T$ $\quad \xi\theta_{w2}(0) = [0\ 0\ 0]^T$

$p_{w3} = [0\ 0\ \ -5]^T$ $\quad \xi\theta_{w3}(0) = \begin{bmatrix}0 & -\frac{\pi}{4} & 0\end{bmatrix}^T$

$p_{w4} = [-5\ \ -5\ \ -5]^T$ $\quad \xi\theta_{w4}(0) = \begin{bmatrix}0 & \frac{\pi}{3} & 0\end{bmatrix}^T$

$p_{w5} = [-5\ 0\ \ -10]^T$ $\quad \xi\theta_{w5}(0) = [0\ 0\ 0]^T$

[m] [rad]

Tracking Performance

$$\|x_e\|_{\mathcal{L}_2} \leq \gamma \|\omega^b_{w1}\|_{\mathcal{L}_2} + \delta$$

(i) $\gamma = 2$

$k_{21} = 2.73,\ k_{32} = 4.45,$
$k_{42} = 5.69,\ k_{54} = 8.38,$
$k_{e21} = 3.37,\ k_{e32} = 3.94,$
$k_{e21} = 6.65,\ k_{e32} = 7.72$

(ii) $\gamma = 0.49$ (better performance)

$k_{21} = 11.28,\ k_{32} = 19.93,$
$k_{42} = 18.99,\ k_{54} = 19.99,$
$k_{e21} = 19.98,\ k_{e32} = 19.92,$
$k_{e21} = 19.99,\ k_{e32} = 19.99$

Simulation Results

Leader's Body Angular Velocity

$$\omega^b_{w1} = \begin{cases} [0\ 0.1\ 0]^T & t \in [0,5) \\ [-0.1\ 0\ 0]^T & t \in [5,10) \\ [0\ -0.1\ 0]^T & t \in [10,20) \\ [0\ 0\ 0]^T & t \in [20,30) \end{cases} \quad \text{[rad/s]}$$

Synchronization

Visibility Structure

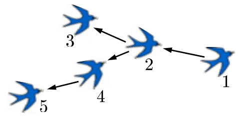

Positions in Σ_w

(i)

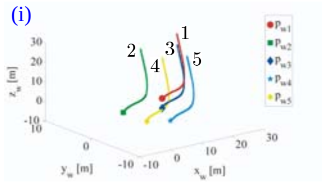

(ii)

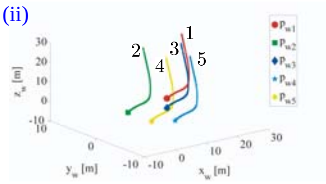

Good Tracking and Synchronization !

Simulation Results

Rotation Angle Errors

(i)

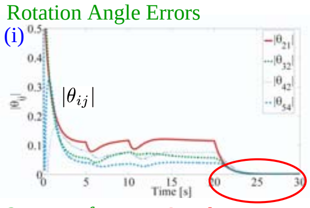

(ii)

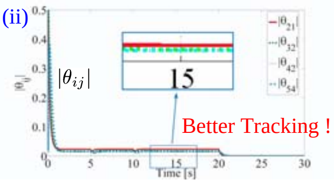

2-norm of x_e Synchronization !

(i)

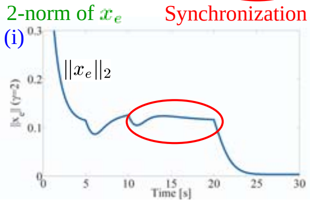

(ii)

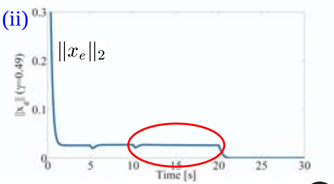

Outline

- Introduction
- Visual Robotic Network
- Visual Feedback Attitude Synchronization
- Tracking Performance
- Simulation
- Conclusion and Future Works

Conclusion and Future Work

Conclusions

- Proposal of Visual Robotic Network
- Proposal of vision-based attitude synchronization law
- Proof of visual feedback attitude synchronization
- Analysis of tracking performance
- Simulation and experiment for verification

Future Works

- Bidirectional visibility (too difficult: local report)
- Tracking performance analysis of visual feedback pose synchronization
- Panoramic camera model
- Rigid bodies with actuators (dynamics)